Pre-existing and de novo humoral immunity to SARS-CoV-2 in humans

Kevin W. Ng[1*], Nikhil Faulkner[1*], Georgina H. Cornish[1*], Annachiara Rosa[2*], Ruth Harvey[3], Saira Hussain[3], Rachel Ulferts[9], Christopher Earl[4], Antoni G. Wrobel[5], Donald J. Benton[5], Chloe Roustan[6], William Bolland[1], Rachael Thompson[1], Ana Agua-Doce[7], Philip Hobson[7], Judith Heaney[13], Hannah Rickman[13], Stavroula Paraskevopoulou[13], Catherine F. Houlihan[13,14], Kirsty Thomson[13], Emilie Sanchez[13], Gee Yen Shin[13], Moira J. Spyer[13,15], Dhira Joshi[8], Nicola O'Reilly[8], Philip A .Walker[6], Svend Kjaer[6], Andrew Riddell[7], Catherine Moore[16], Bethany R. Jebson[17,19], Meredyth G.Ll. Wilkinson[17,19], Lucy R. Marshall[17,19], Elizabeth C. Rosser[17,18], Anna Radziszewska[17,18], Hannah Peckham[17,18], Coziana Ciurtin[17,18], Lucy R. Wedderburn[17,19], Rupert Beale[9], Charles Swanton[10], Sonia Gandhi[11], Brigitta Stockinger[12], John McCauley[3], Steve J. Gamblin[5], Laura E. McCoy[14]†, Peter Cherepanov[2]†, Eleni Nastouli[13,15]† and George Kassiotis[1,20]†

[1]Retroviral Immunology; [2]Chromatin structure and mobile DNA Laboratory; [3]Worldwide Influenza Centre; [4]Signalling and Structural Biology Laboratory; [5]Structural Biology of Disease Processes Laboratory; [6]Structural Biology STP; [7]Flow Cytometry STP; [8]Peptide Chemistry; [9]Cell Biology of Infection Laboratory; [10]Cancer Evolution and Genome Instability Laboratory; [11]Neurodegeneration Biology Laboratory; [12]AhRimmunity Laboratory, The Francis Crick Institute, 1 Midland Road, London NW1 1AT, UK

[13]University College London Hospitals (UCLH) NHS Trust, London NW1 2BU, UK

[14]Division of Infection and Immunity, University College London (UCL), London WC1E 6BT, UK

[15]Department of Population, Policy and Practice, Great Ormond Street Institute for Child Health (ICH), UCL, London WC1N 1EH, UK

[16]Public Health Wales, University Hospital of Wales, Cardiff CF14 4XW, UK

[17]Centre for Adolescent Rheumatology Versus Arthritis at UCL, UCLH, Great Ormond Street Hospital (GOSH); [18]Centre for Rheumatology Research, Division of Medicine, UCL, London, UK

[19]UCL Great Ormond Street Institute for Child Health (ICH), UCL, London, UK

[20]Department of Medicine, Faculty of Medicine, Imperial College London, London W2 1PG, UK

†Correspondence:

George Kassiotis, george.kassiotis@crick.ac.uk;

Eleni Nastouli, e.nastouli@ucl.ac.uk;

Peter Cherepanov, peter.cherepanov@crick.ac.uk;

Laura E. McCoy, l.mccoy@ucl.ac.uk.

*Equal contribution

Abstract

Zoonotic introduction of novel coronaviruses may encounter pre-existing immunity in humans. Using diverse assays for antibodies recognizing SARS-CoV-2 proteins, we detect pre-existing humoral immunity. SARS-CoV-2 spike glycoprotein (S)-reactive antibodies were detectable by a flow cytometry-based method in SARS-CoV-2-uninfected individuals and were particularly prevalent in children and adolescents. They were predominantly of the IgG class and targeted the S2 subunit. By contrast, SARS-CoV-2 infection induced higher titers of SARS-CoV-2 S-reactive IgG antibodies, targeting both the S1 and S2 subunits, and concomitant IgM and IgA antibodies, lasting throughout the observation period. Notably, SARS-CoV-2-uninfected donor sera exhibited specific neutralizing activity against SARS-CoV-2 and SARS-CoV-2 S pseudotypes. Distinguishing pre-existing and de novo immunity will be critical for our understanding of susceptibility to and the natural course of SARS-CoV-2 infection.

Immune cross-reactivity among seasonally spreading human coronaviruses (HCoVs) has long been hypothesized to provide effective, but transient cross-protection against distinct HCoVs (*1*, *2*). To determine the degree of cross-reactivity between HCoVs and SARS-CoV-2, we developed a flow cytometry-based assay for SARS-CoV-2-binding antibodies. The main target for such antibodies is the spike glycoprotein (S), which is proteolytically processed into the S1 and S2 subunits, mediating target cell attachment and entry, respectively.

The S1-specific CR3022 antibody stained a smaller percentage of SARS-CoV-2 S-expressing HEK293T cells and with lower intensity than COVID-19 convalescent sera (fig. S1), indicating that polyclonal IgG antibodies targeted a wider range of epitopes naturally processed and displayed on these cells. This assay also detected SARS-CoV-2 S-reactive IgM and IgA antibodies in COVID-19 convalescent sera (fig. S2). Indeed, the presence of SARS-CoV-2 S-reactive antibodies of all three Ig classes ($IgG^+IgM^+IgA^+$) distinguished COVID-19 sera from control sera with a high degree of sensitivity and specificity (Fig. 1A and fig. S3). All 156 seroconverted COVID-19 patients had contemporaneous IgG, IgM, and IgA responses to SARS-CoV-2 S throughout the observation period, with the exception of two patients, who only had IgG antibodies (fig. S4 and S5). One of these patients was a bone-marrow-transplant recipient who experienced HCoV infection a month prior to SARS-CoV-2 infection (fig. S6). Remarkably, a small proportion of SARS-CoV-2-uninfected patients, sampled before or during the early spread of SARS-CoV-2 in the UK (Table S1), also had SARS-CoV-2 S-binding IgG, but not IgM or IgA antibodies (Fig. 1A), suggesting the presence of cross-reactive immunological memory.

The S2 subunit exhibits a higher degree of homology among coronaviruses than S1 (fig. S7) and was likely the main target of cross-reactive antibodies. Competition with recombinant soluble S1 or S2, at doses that blocked binding of specific monoclonal antibodies (Fig. S8), did not affect the frequency of cells stained with COVID-19 patient sera, although the intensity of staining was reduced by 31% and 37%, respectively (Fig. 1, B to D), indicating recognition of both S1 and S2. By contrast, soluble S2 completely abolished staining with SARS-CoV-2-uninfected patient sera, whereas soluble S1 had no effect (Fig. 1, B to D). Thus, SARS-CoV-2-uninfected patient sera cross-reacts with SARS-CoV-2 S2 and COVID-19 patient sera additionally recognizes S1.

SARS-CoV-2 S-reactive IgG antibodies were detected by flow cytometry in 5 of 34 SARS-CoV-2-uninfected individuals with RT-qPCR-confirmed HCoV infection, as well as in 1 of 31 individuals without recent HCoV infection (Fig. 2A and fig. S4A). This suggested that cross-reactivity may have persisted from earlier HCoV infections, rather than having been induced by the most recent one.

To confirm antibody cross-reactivity using an independent assay, we developed ELISAs using recombinant SARS-CoV-2 stabilized trimeric S ectodomain, S1, receptor-binding domain (RBD), or nucleoprotein (N). Rates of IgG seropositivity by SARS-CoV-2 S1-coated ELISA were congruent with, but generally lower than those by flow cytometry (fig. S9). The three SARS-CoV-2-uninfected individuals with the highest cross-recognition of S by flow cytometry, plus an additional four individuals, had ELISA-detectable IgG antibodies against SARS-CoV-2 S ectodomain, as well as N (Fig. 2A and fig. S4, B to D). By contrast, none of the control samples had ELISA-detectable IgG antibodies against the less conserved SARS-CoV-2 S1 or RBD (Fig. 2A and fig. S4, B to D).

The prevalence of such cross-reactive antibodies was further examined in additional healthy donor cohorts (Table S1). Among 50 SARS-CoV-2-uninfected pregnant women, sampled in May 2018, five showed evidence for SARS-CoV-2 S-reactive IgG, but not IgM or IgA antibodies (Fig. 2B and fig. S10). In a separate cohort of 101 SARS-CoV-2-uninfected donors, sampled in May 2019, three had SARS-CoV-2 S-reactive IgG antibodies (fig. S11),

which did not correlate with antibodies to diverse viruses and bacteria also present in several of these samples. SARS-CoV-2 S-reactive IgM and IgA were also detected in two of these donors, albeit at considerably lower levels than in COVID-19 patients (fig. S11), suggestive of recent or ongoing response. In an additional cohort of 13 donors recently infected with HCoVs, only one had SARS-CoV-2 S-reactive IgG antibodies, and these at very low levels (fig. S12). This suggested that their emergence was not simply a common transient event following each HCoV infection in this age group (median age 51 years; Table S1). Instead, given that HCoV-reactive antibodies are present in virtually all adults (*3-5*), the rarity of SARS-CoV-2 S cross-reactivity (16 of 302; 5.29%), indicates additional requirements, such as random B cell receptor repertoire focusing or frequency of HCoV infection, rather than time since the last HCoV infection. Indeed, the frequency of HCoV infection displays a characteristic age distribution, being the highest in children and adolescents (*1, 4-8*). We therefore examined a cohort of younger SARS-CoV-2-uninfected healthy donors (aged 1-16 years; Table S1), sampled between 2011 and 2018. Remarkably, at least 21 of these 48 donors had detectable levels of SARS-CoV-2 S-reactive IgG antibodies (Fig. 2, C to E), whereas only one of an additional cohort of 43 young adults (aged 17-25 years; Table S1) had such antibodies (Fig. 2F). Staining with sera from SARS-CoV-2-uninfected children and adolescents was specific to HEK293T cells expressing SARS-CoV-2 S, but not the unrelated HERV-K113 envelope glycoprotein, and was outcompeted by soluble SARS-CoV-2 S2 (fig. S13). The prevalence of SARS-CoV-2 S-reactive IgG antibodies peaked at 62% between 6 and 16 years of age (Fig. 2F), when HCoV seroconversion in this age group also peaks (*3, 4, 6, 7*), and was significantly higher than in adults ($P<0.00001$, Fisher's exact test).

To probe the potential consequences of antibody cross-reactivity, we examined the ability of pre-existing antibodies to inhibit SARS-CoV-2 entry into HEK293T cells (fig. S14 and supplementary text). Although not expected to directly inhibit RBD-mediated cell attachment, S2-targeting antibodies that can neutralize SARS-CoV-2 have recently been discovered (*9, 10*). HEK293T cell infection with SARS-CoV-2 S pseudotypes was efficiently inhibited by sera from seroconverted (Ab^+) COVID-19 patients, but not from those that had not yet seroconverted (Ab^-) (Fig. 3A). Surprisingly, sera from SARS-CoV-2-uninfected donors with SARS-CoV-2 S-reactive antibodies also neutralized these pseudotypes, whereas none of the sera neutralized vesicular stomatitis virus (VSV) glycoprotein pseudotypes (Fig. 3A). Comparable neutralization of SARS-CoV-2 S pseudotypes was also observed with sera from SARS-CoV-2-uninfected adolescents (Fig. 3A). Moreover, the majority of sera from SARS-CoV-2-uninfected donors with flow cytometry-detectable cross-reactive antibodies also neutralized authentic SARS-CoV-2 infection of Vero E6 cells, albeit on average less potently than COVID-19 patient sera (Fig. 3B). By contrast, sera from SARS-CoV-2-uninfected patients without cross-reactive antibodies exhibited no neutralizing activity (Fig. 3B). Antiviral antibodies may also enhance viral entry by Fc receptor-mediated antibody-dependent enhancement (ADE). However, entry of SARS-CoV-2 S pseudotypes was not enhanced by either COVID-19 patient or SARS-CoV-2-uninfected patient sera in FcγRIIA-expressing K-562 cells (fig. S15).

Collectively, these findings highlighted functionally relevant antigenic epitopes conserved within the S2. Over its entire length, SARS-CoV-2 S exhibits marginally closer homology with the S proteins of betacoronaviruses HCoV-OC43 and HCoV-HKU1, than of alphacoronaviruses HCoV-NL63 and HCoV-229E (fig. S16A). To probe shared epitopes, we constructed overlapping peptide arrays spanning the last 743 amino acids of SARS-CoV-2 S (fig. S16B). Multiple putative epitopes were differentially recognized by sera with cross-reactive antibodies (Ab^+), were reasonably conserved, and most mapped to the surface of S2 (Fig. 4, A and B, and Table S2). Of note, an epitope overlapping the S2 fusion peptide was also recently identified as cross-reactive with the corresponding peptides from HCoV-OC43

and HCoV-229E (*11*). Cross-reactivity with the identified epitopes was further supported by ELISAs coated with synthetic peptides (fig. S17).

As expected (*3-5*), reactivity with one or more HCoVs was detectable by flow cytometry in all sera (Fig. 4D and fig. S18). However, IgG and IgA reactivity against HCoVs was higher in SARS-CoV-2-uninfected adults with, than without SARS-CoV-2-reactive IgG (P=1.4×10^{-6} for IgG and P=0.017 for IgA, Student's t test), and in SARS-CoV-2-uninfected children or adolescents with, than without SARS-CoV-2-reactive IgG (P=0.010 for IgG and P=0.021 for IgA, Student's t test) (Fig. 4D), supporting a direct link between the two. Accordingly, IgG reactivity against each HCoV type was independently correlated with the presence of SARS-CoV-2-reactive antibodies (Fig. 4D).

Our results from multiple independent assays demonstrated the presence of pre-existing antibodies recognizing SARS-CoV-2 in uninfected individuals. Identification of conserved epitopes in S2 targeted by neutralizing antibodies may hold promise for a universal vaccine protecting against current, as well as future CoVs. Together with pre-existing T cell (*12-14*) and B cell memory (*10*, *15*), antibody cross-reactivity between seasonal HCoVs and SARS-CoV-2 may have important ramifications for natural infection. Epidemiological studies of HCoV transmission suggest that cross-protective immunity is unlikely to be sterilizing or long-lasting (*8*), which is also supported by repeated reinfection (*2*, *16*). Nevertheless, prior immunity induced by one HCoV can reduce the transmission of homologous and heterologous HCoVs, and ameliorate the symptoms where transmission is not prevented (*1*, *2*). A possible modification of COVID-19 severity by prior HCoV infection may account for the age distribution of COVID-19 susceptibility, where higher HCoV infection rates in children than in adults (*4*, *6*) correlates with relative protection from COVID-19 (*17*) and may also shape seasonal and geographical patterns of transmission. It is, therefore, imperative that any effect, positive or negative, of pre-existing HCoV-elicited immunity on the natural course of SARS-CoV-2 infection be fully delineated.

References

1. R. W. Aldridge *et al.*, Seasonality and immunity to laboratory-confirmed seasonal coronaviruses (HCoV-NL63, HCoV-OC43, and HCoV-229E): results from the Flu Watch cohort study. *Wellcome Open Research* **5**, (2020).
2. K. A. Callow, H. F. Parry, M. Sergeant, D. A. Tyrrell, The time course of the immune response to experimental coronavirus infection of man. *Epidemiology and infection* **105**, 435-446 (1990).
3. E. G. Severance *et al.*, Development of a nucleocapsid-based human coronavirus immunoassay and estimates of individuals exposed to coronavirus in a U.S. metropolitan population. *Clinical and vaccine immunology : CVI* **15**, 1805-1810 (2008).
4. R. Dijkman *et al.*, Human coronavirus NL63 and 229E seroconversion in children. *Journal of clinical microbiology* **46**, 2368-2373 (2008).
5. A. T. Huang *et al.*, A systematic review of antibody mediated immunity to coronaviruses: kinetics, correlates of protection, and association with severity. *Nature communications* **11**, 4704 (2020).
6. N. Friedman *et al.*, Human Coronavirus Infections in Israel: Epidemiology, Clinical Symptoms and Summer Seasonality of HCoV-HKU1. *Viruses* **10**, (2018).
7. S. Nickbakhsh *et al.*, Epidemiology of seasonal coronaviruses: Establishing the context for COVID-19 emergence. *The Journal of infectious diseases*, (2020).
8. A. S. Monto *et al.*, Coronavirus occurrence and transmission over 8 years in the HIVE cohort of households in Michigan. *The Journal of infectious diseases*, (2020).
9. X. Chi *et al.*, A neutralizing human antibody binds to the N-terminal domain of the Spike protein of SARS-CoV-2. *Science (New York, N.Y.)*, eabc6952 (2020).
10. G. Song *et al.*, Cross-reactive serum and memory B cell responses to spike protein in SARS-CoV-2 and endemic coronavirus infection. *bioRxiv*, 2020.2009.2022.308965 (2020).
11. E. Shrock *et al.*, Viral epitope profiling of COVID-19 patients reveals cross-reactivity and correlates of severity. *Science (New York, N.Y.)*, eabd4250 (2020).
12. A. Grifoni *et al.*, Targets of T cell responses to SARS-CoV-2 coronavirus in humans with COVID-19 disease and unexposed individuals. *Cell*, (2020).
13. J. Braun *et al.*, SARS-CoV-2-reactive T cells in healthy donors and patients with COVID-19. *Nature*, (2020).
14. N. Le Bert *et al.*, SARS-CoV-2-specific T cell immunity in cases of COVID-19 and SARS, and uninfected controls. *Nature*, (2020).
15. P. Nguyen-Contant *et al.*, S Protein-Reactive IgG and Memory B Cell Production after Human SARS-CoV-2 Infection Includes Broad Reactivity to the S2 Subunit. *mBio* **11**, e01991-01920 (2020).
16. P. K. Kiyuka *et al.*, Human Coronavirus NL63 Molecular Epidemiology and Evolutionary Patterns in Rural Coastal Kenya. *The Journal of infectious diseases* **217**, 1728-1739 (2018).
17. R. Castagnoli *et al.*, Severe Acute Respiratory Syndrome Coronavirus 2 (SARS-CoV-2) Infection in Children and Adolescents: A Systematic Review. *JAMA pediatrics*, (2020).

Acknowledgements

We thank L. James and J. Luptak for the SARV CoV2 N expression construct and M. Pizzato for the SARS CoV2 S cDNA. We also thank the entire CRICK COVID-19 Consortium. We are grateful for assistance from the Cell Services and High Throughput Screening facilities at the Francis Crick Institute and UCLH Biochemistry (A. Goyale and C. Wilson) and to Mr Michael Bennet and Mr Simon Caidan for training and support in the high-containment laboratory. **Funding**: This work was supported by a Centre of Excellence Centre for Adolescent Rheumatology Versus Arthritis grant, 21593, as well as support from the Great Ormond Street Childrens Charity, CureJM Foundation and the NIHR Biomedical Research Centres at GOSH and UCLH. This work was supported by the Francis Crick Institute, which receives its core funding from Cancer Research UK, the UK Medical Research Council, and the Wellcome Trust. **Author contributions:** Experimental design, C.C., L.R.W., R.B., C.S., S.G., B.S., J.McC., S.J.G., L.E.McC., P.C., E.N., and G.K. Investigation, K.W.N., N.F., G.H.C., A.Ro., R.H., S.H., R.U., C.E., A.G.W., D.J.B., C.R., W.B., R.T., A.A.-D., P.H., and D.J. Reagents and Samples, J.H., H.R., S.P., C.F.H., K.T., E.S., G.Y.S., M.J.S., P.A.W., C.M., B.R.J., M.G.Ll.W., L.R.M., E.C.R., A.Ra., and H.P. Writing, L.E.McC., P.C., E.N., and G.K., with contributions from C.C., L.R.W., K.W.N., N.F., and G.H.C. Supervision, N.O'R., S.K., A.Ri., C.C., L.R.W., R.B., C.S., S.G., B.S., J.McC., S.J.G., L.E.McC., P.C., E.N., and G.K. **Competing interests:** The authors declare no competing interests. **Data and materials availability:** All data are available in the main text or the supplementary materials.
This work is licensed under a Creative Commons Attribution 4.0 International (CC BY 4.0) license, which permits unrestricted use, distribution, and reproduction in any medium, provided the original work is properly cited. To view a copy of this license, visit https://creativecommons.org/licenses/by/4.0/. This license does not apply to figures/photos/artwork or other content included in the article that is credited to a third party; obtain authorization from the rights holder before using such material.

Figure legends

Fig. 1. Flow cytometric detection and specificity of antibodies reactive with SARS-CoV-2 S. (**A**) Detection of IgG, IgA, and IgM in five individuals from each indicated group. IgM levels are indicated by a heatmap. (**B** to **D**) Inhibition of SARS-CoV-2 S binding of sera from SARS-CoV-2-infected (SARS-CoV-2^+, n=10) or SARS-CoV-2-uninfected (SARS-CoV-2^- $HCoV^+$, n=6) patients by soluble S1 or S2. Flow cytometry profile of one representative patient per group is shown (B). Mean frequency of positive cells (C). **P*=0.015; ***P*=0.006, one-way analysis of variance (ANOVA) on Ranks. Mean staining intensity (mean fluorescent intensity (MFI) of sample as a percentage of negative control MFI) (D). In C and D, dots represent individual samples from one of three similar experiments.

Fig. 2. Prevalence of SARS-CoV-2 S-cross-reactive antibodies detected by different methods. (**A**) Flow cytometry and ELISA results for each sample in cohorts A and C to E (table S1). (**B**) Flow cytometry and ELISA results for serum samples from SARS-CoV-2-uninfected pregnant women. (**C** to **E**) SARS-CoV-2 S-cross-reactive antibodies in healthy children and adolescents. Representative flow cytometry profiles of seronegative donors (Negative) or COVID-19 patients (Positive) and of SARS-CoV-2-uninfected adolescents with SARS-CoV-2-cross-reactive antibodies (C). Frequency of cells stained with all three antibody classes ($IgG^+IgM^+IgA^+$) or only with IgG (IgG^+), ranked by their $IgG^+IgM^+IgA^+$ frequency (D). The dashed line denotes the assay sensitivity cut-off. Flow cytometry and ELISA results for each sample (E). (**F**) Prevalence of SARS-CoV-2 S-cross-reactive antibodies in the indicated age groups (line) and frequency of cells that stained only with IgG (dots) in all samples for which the date of birth was known. The heatmaps in A, B, and E represent the quartile values above each assay's technical cut-off.

Fig. 3. Neutralization of SARS-CoV-2 S pseudotypes and authentic SARS-CoV-2 by SARS-CoV-2-infected and -uninfected patient sera. (**A**) Inhibition of transduction efficiency of SARS-CoV-2 S or VSVg pseudotypes by adult COVID-19 patients who seroconverted (SARS-CoV-2^+ Adults Ab^+) or not (SARS-CoV-2^+ Adults Ab^-), and SARS-CoV-2-uninfected adult (SARS-CoV-2^- Adults Ab^+) or children and adolescent donors (SARS-CoV-2^- Children/Adolescents Ab^+) donors with SARS-CoV-2 S-binding antibodies. Each line is an individual serum sample. (**B**) Authentic SARS-CoV-2 neutralization titers of sera from the same donors as in A, as well as SARS-CoV-2-uninfected donors without SARS-CoV-2 S-binding antibodies (Ab^-). Dots represent individual samples. **P*=0.037; ***P*=0.014; ns: not significant, one-way ANOVA on Ranks.

Fig. 4. Mapping of cross-reactive epitopes in SARS-CoV-2 S. (**A**) Signal intensity for each overlapping peptide along the length of SARS-CoV-2 S covered in the peptide arrays, using pooled sera with (Ab^+) or without (Ab^-) flow cytometry-detectable SARS-CoV-2 S-reactive antibodies. Differentially recognized peaks are boxed. (**B**) Alignment of the amino acid sequences of SARS-CoV-2 and HCoV S glycoproteins. Boxes indicate predicted core epitopes. (**C**) Mapping of predicted epitopes targeted on the trimeric SARS-CoV-2 spike. The S1 (blue) and S2 (pink) of one monomer are colored. Epitopes are shown for one monomer; the circled dashed line represent the membrane proximal region not present in the structure. (**D**) (Left), Reactivity with the S glycoproteins of each HCoV of the indicated sera with (Ab^+) or without (Ab^-) flow cytometry-detectable SARS-CoV-2 S-reactive antibodies, determined by flow cytometry. Each column is an individual sample. Rows depict the staining for each antibody class. (Right), Correlation coefficients between percentages of IgG staining for SARS-CoV-2 S and IgG, IgM, and IgA staining for each HCoV S glycoprotein.

Figure 1

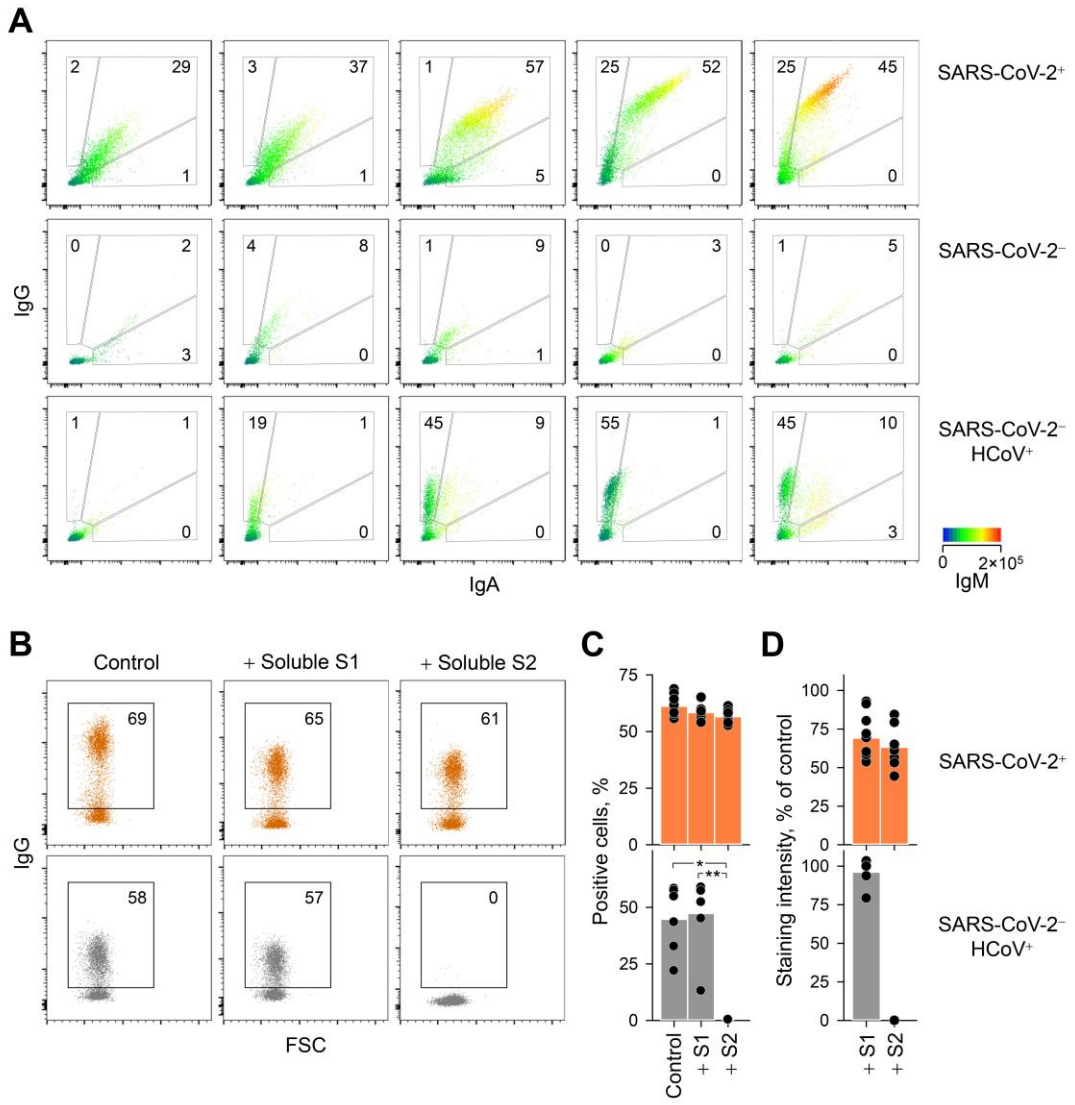
A
SARS-CoV-2+
SARS-CoV-2−
SARS-CoV-2− HCoV+
IgG
IgA
0
2×10^5
IgM
B
Control
+ Soluble S1
+ Soluble S2
IgG
FSC
C
Positive cells, %
Control
+ S1
+ S2
D
Staining intensity, % of control
+ S1
+ S2

Figure 2

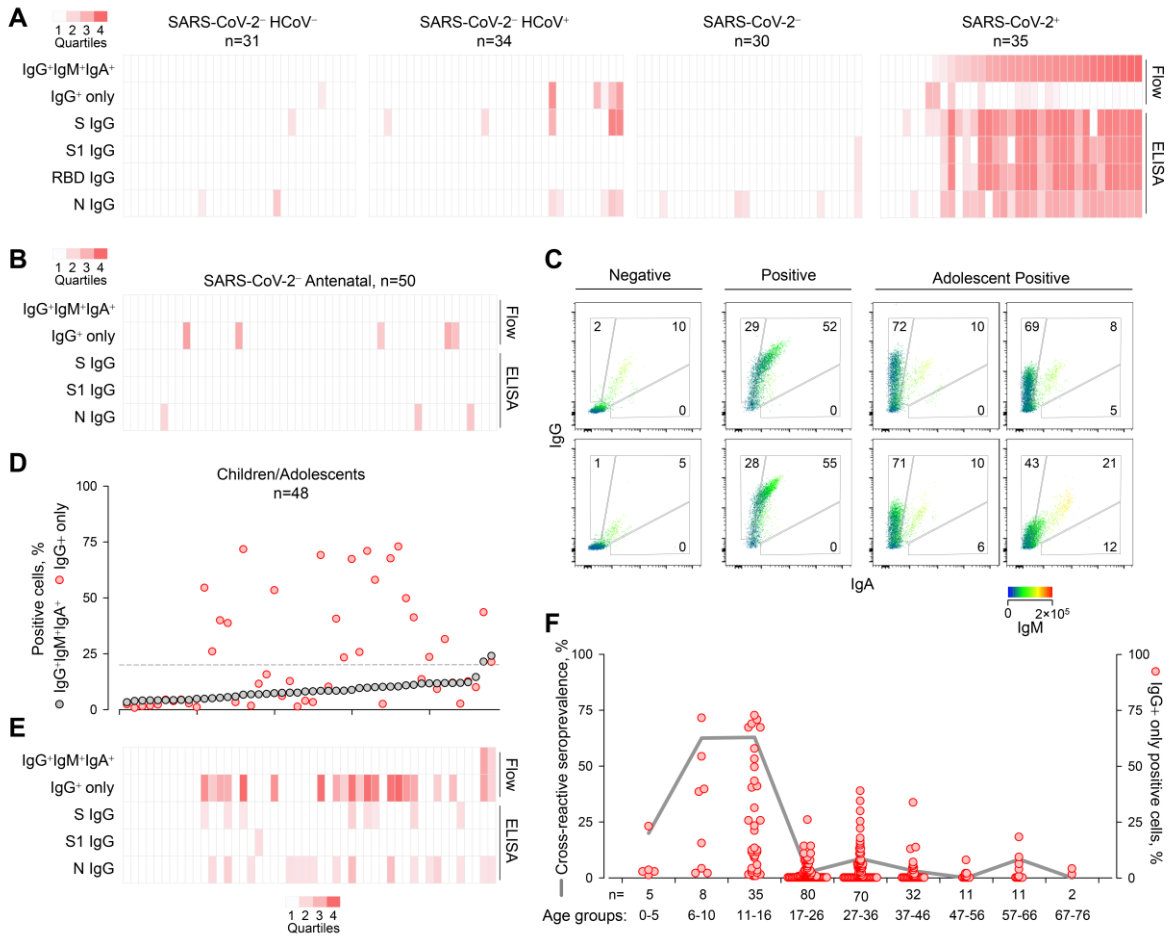
A
1 2 3 4 Quartiles
SARS-CoV-2⁻ HCoV⁻ n=31
SARS-CoV-2⁻ HCoV⁺ n=34
SARS-CoV-2⁻ n=30
SARS-CoV-2⁺ n=35
IgG⁺IgM⁺IgA⁺
IgG⁺ only
S IgG
S1 IgG
RBD IgG
N IgG
Flow
ELISA
B
SARS-CoV-2⁻ Antenatal, n=50
C
Negative
Positive
Adolescent Positive
IgG
IgA
IgM
D
Children/Adolescents n=48
Positive cells, %
E
F
Cross-reactive seroprevalence, %
IgG+ only positive cells, %
n= 5 8 35 80 70 32 11 11 2
Age groups: 0-5 6-10 11-16 17-26 27-36 37-46 47-56 57-66 67-76

Figure 3

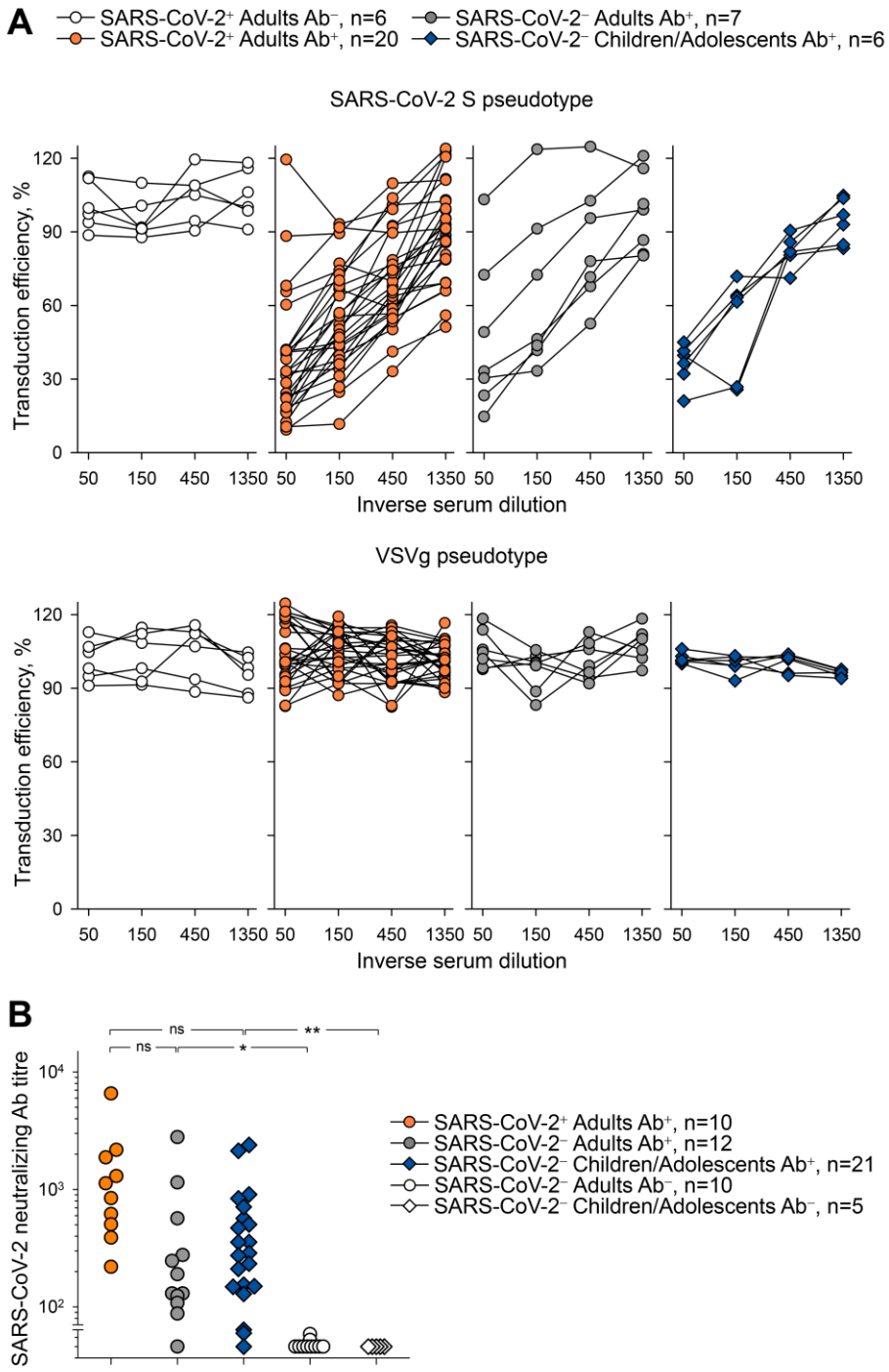
A
SARS-CoV-2+ Adults Ab−, n=6
SARS-CoV-2+ Adults Ab+, n=20
SARS-CoV-2− Adults Ab+, n=7
SARS-CoV-2− Children/Adolescents Ab+, n=6
SARS-CoV-2 S pseudotype
Transduction efficiency, %
Inverse serum dilution
VSVg pseudotype
B
SARS-CoV-2 neutralizing Ab titre
ns
ns
*
**
SARS-CoV-2+ Adults Ab+, n=10
SARS-CoV-2− Adults Ab+, n=12
SARS-CoV-2− Children/Adolescents Ab+, n=21
SARS-CoV-2− Adults Ab−, n=10
SARS-CoV-2− Children/Adolescents Ab−, n=5

Figure 4

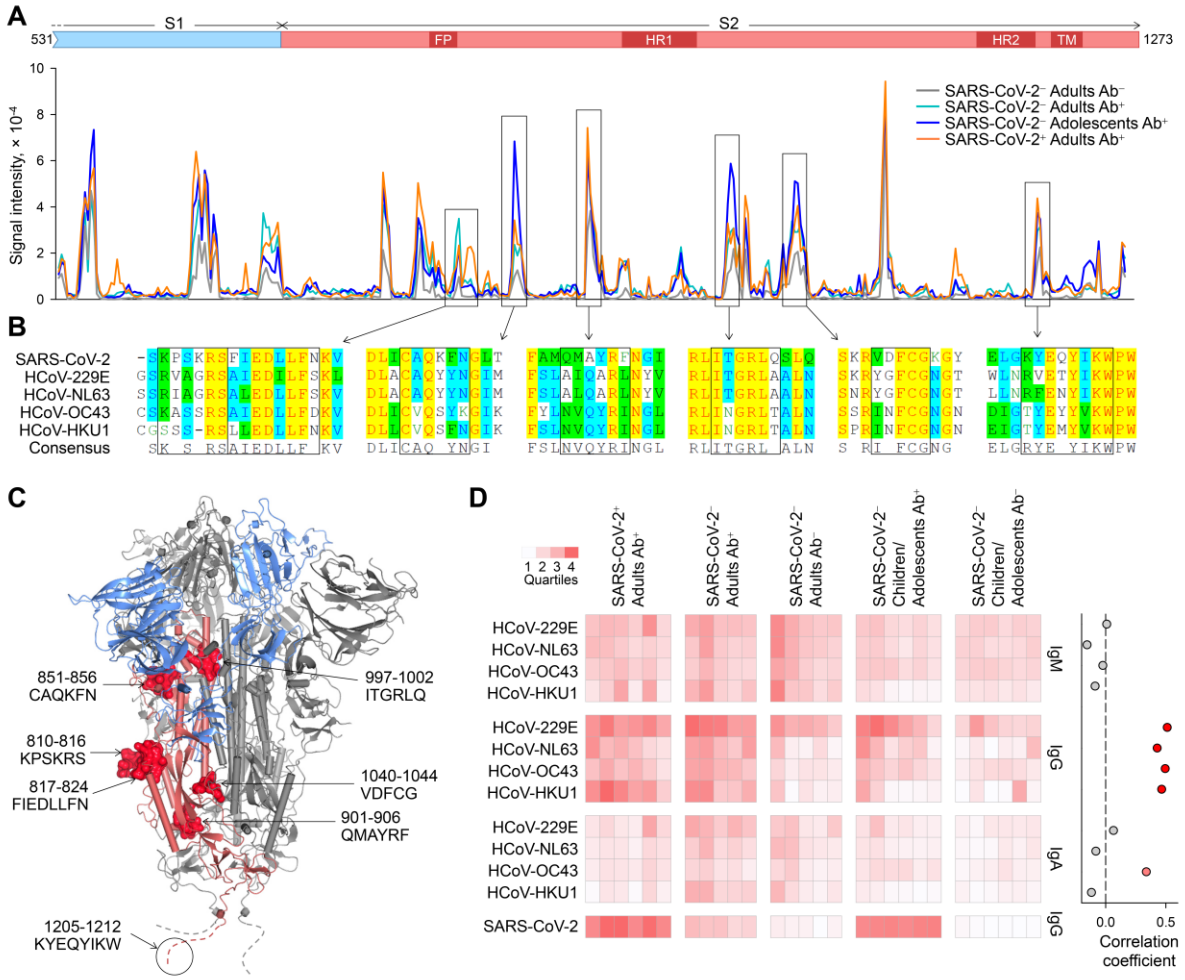
A
S1
S2
531
1273
FP
HR1
HR2
TM
Signal intensity, × 10⁻⁴
SARS-CoV-2⁻ Adults Ab⁻
SARS-CoV-2⁻ Adults Ab⁺
SARS-CoV-2⁻ Adolescents Ab⁺
SARS-CoV-2⁺ Adults Ab⁺
B
SARS-CoV-2
HCoV-229E
HCoV-NL63
HCoV-OC43
HCoV-HKU1
Consensus
C
851-856
CAQKFN
997-1002
ITGRLQ
810-816
KPSKRS
1040-1044
VDFCG
817-824
FIEDLLFN
901-906
QMAYRF
1205-1212
KYEQYIKW
D
1 2 3 4
Quartiles
SARS-CoV-2⁺ Adults Ab⁺
SARS-CoV-2⁻ Adults Ab⁺
SARS-CoV-2⁻ Adults Ab⁻
SARS-CoV-2⁻ Children/ Adolescents Ab⁺
SARS-CoV-2⁻ Children/ Adolescents Ab⁻
HCoV-229E
HCoV-NL63
HCoV-OC43
HCoV-HKU1
SARS-CoV-2
IgM
IgG
IgA
IgG
0.0
0.5
Correlation coefficient